

WORKING TITLE:

Quanteneffekte, Wasser auf Metalloxidoberflächen

Dissertation zur Erlangung des akademischen Grades
›doctor rerum naturalium‹ (Dr. rer. nat.)
in der Wissenschaftsdisziplin Theoretische Chemie

vorgelegt von
Sophia L. Heiden

an der
Mathematisch-Naturwissenschaftlichen Fakultät
der Universität Potsdam



Potsdam, xx 2018

This work has been done between January 2015 and xx 2018 in the workgroup of Prof. Dr. Peter Saalfrank at the Institute of Chemistry at the University of Potsdam.

Potsdam, xx 2018

Erstgutachter: Prof. Dr. Peter Saalfrank

Zweitgutachter: Prof. Dr. Beate Paulus

Drittgutachter: Prof. Dr. xy

Preamble

The importance of surface science in our industrialized world is overwhelming, because most processes in industry need (heterogeneous) catalysts, because these do not have to be separated from the reactants and the product after the process, which is mostly a costly step in the production of chemicals. It is therefore desirable to understand heterogeneous catalytic processes by learning more about the processes that take place on the surface of materials. Metal oxide materials are frequently used in catalysts as well as catalyst support materials, so that understanding their properties in contact with chemicals, in this work water, is crucial.

Aluminum is used in rocket fuels as a reduction agent so that during launch alumina particles are ejected in the atmosphere during the start (see also lit.dat!). For a space shuttle the start can produce around 760,000 kg of alumina particles. It can be measured that approximately one third of these particles can be deposited in the stratosphere (in an altitude between 15 and 50 km above the surface of the earth) and there it can react with the water and other molecules in the stratosphere where these particles are accumulated after the launch of a shuttle.

Also in geochemical sciences Al_2O_3 is a subject of a variety of studies since aluminum is the third most common element in the crust with 6.3% (

http://www.unterra.de/rutherford/tab_hauf.htm

check also dtv atlas der chemie band 1!) and it also can be seen as a model systems for more complex aluminosilicates. Oxide rocks are omnipresent in the crust of the earth and henceforth in most geochemical processes since the times the earth's atmosphere became oxidizing with rise of photosynthetic life forms/(bacteria?) a few million years ago. Before under reductive conditions sulfidic rocks were dominant but when photosynthesis became more common with the rise of more advanced life forms, the oxygen content of the atmosphere grew.

Contents

Preamble	3
1 Theory und Methodology	7
1.1 DFT	7
1.2 Periodic Boundary Conditions	8
1.3 Atom Centered Basis and Peculiarities	9
1.4 <i>Ab-initio</i> Molecular Dynamics	9
1.5 Frequencies and Intensities	9
1.6 Finding Transition States	10
1.7 From Density Functionals to Hybrids and Perturbation Theory	11
1.8 Computational Details and Used Programs	11
1.9 Experimental Techniques	12
1.9.1 Vibrational Sum Frequency Generation	12
1.9.2 Thermal Desorption Spectroscopy	12
1.9.3 Molecular Beam Source vs. Pinhole Dosing	12
1.9.4 Low-Energy Electron Diffraction	13
2 Water on $\alpha\text{-Al}_2\text{O}_3(11\bar{2}0)$	15
2.1 Surface Model	15
2.2 Structure Search	17
2.3 Reactions and Microkinetic Model	19
2.4 Vibrational Frequencies / Spectroscopic Properties	24
2.4.1 OH/OD Vibrations	25
2.4.2 Lattice Vibrations	26
2.5 Desorption Process	26
3 Water on $\alpha\text{-Al}_2\text{O}_3(0001)$	27
3.1 Surface Model	27
3.2 AIMD for Dissociation Process	27
3.2.1 Microcanonical	30

Contents

3.2.2	Canonical	30
3.3	Improvement of Reaction Rates	31
3.3.1	MP2 and B3LYP	31
3.3.2	PIMD	32
3.3.3	QM/QM Embedding Scheme	32
Summary		33
Appendix		35
References		39

1 Theory und Methodology

In this chapter the basics of the applied theoretical methods shall be explained.

1.1 DFT

basic idea of DFT, only 3 dimensional system instead of 3N-dimensional with N being the number of electrons, Kohn-Sham DFT use orbitals again, methods and algorithms known from wave function based methods can be applied, functionals difference pure density functionals and hybrid, some exact exchange from Hartree Fock is mixed into the potential, functionals like B3LYP, HSE06. Dispersion corrections that account for van-der-Waals interactions, and are important for the adsorbate-surface interaction and the adsorbate-adsorbate interaction.

A test system with non-interacting electrons that reflects the systems electron density, is set and calculated.

Hohenberg-Kohn theorem connect the Hamiltonian of a many-particle system to its ground-state density $n(\mathbf{r})$. If $\Psi(\mathbf{r}^N)$ is an N-electron wavefunction, then the electron density can be given as

$$n(\mathbf{r}) = N \int \dots \int \Psi^*(\mathbf{r}, \mathbf{r}_2, \mathbf{r}_3, \dots, \mathbf{r}_N) \Psi(\mathbf{r}, \mathbf{r}_2, \mathbf{r}_3, \dots, \mathbf{r}_N) d\mathbf{r}_2 \dots d\mathbf{r}_N \quad (1.1)$$

with Hohenberg-Kohn Theorem I the total energy $E[n]$ can be determined as:

$$E[n] = T[n] + V_{ext}[n] + V_{ee}[n] = \int n(\mathbf{r}) v_{ext}(\mathbf{r}) d\mathbf{r} + T[n] + E_H[n] + E_{xc}[n] \quad (1.2)$$

with the kinetic energy $T[n]$, the potential energy $V[n]$ for electron electron interaction ee and external potential ext , the Hartree energy $E_H[n]$, corresponding to the classical Coulomb interaction and the exchange correlation energy $E_{xc}[n]$ for the non-classical exchange correlation interactions.

A problem is, that the explicit form of the interacting kinetic energy $T[n]$ and the exchange correlation functional $E_{xc}[n]$ are unknown.

1.2 Periodic Boundary Conditions

plane wave basis, no atom centered basis functions, periodic boundary conditions, electron density has to be the same in each repeating unit, Miller Indices for nomenclature of surface sites/faces (3 and 4 numbers) (hkl , $hk-(h+k)l$), how to understand these numbers, hexagonal cells, lattice types, differences between these types, Bravais lattice, Brillouin zone, \mathbf{k} -points, irreducible \mathbf{k} -points necessary for describing the system, direct and reciprocal room, how to convert between these two with the lattice vectors

Surface simulation, 2-D system reproduced as 3-D structure since vasp is bulk code there have to be 3 dimensions, so one has to define a vacuum gap between two slabs along the z-axis (perpendicular to the surface) to prevent unit cells from influencing each other and therefore lead to unphysical behaviour. Some programs (here used crystal and cp2k(?)) deliver opportunity to calculate only 2D system, repeating the slab only in x/y, a/b, respectively.

The systems are modelled as periodic solid, this can be described by a unit cell, that is translated along every spatial direction. The lattice can be described by the lattice vector \mathbf{B} . \mathbf{a}_i are basis vectors of the lattice and n_i integers:

$$\mathbf{B} = n_1 \mathbf{a}_1 + n_2 \mathbf{a}_2 + n_3 \mathbf{a}_3 \quad (1.3)$$

Analogue to that, also a reciprocal space exists (\mathbf{k} -space) with a set of vectors \mathbf{G} :

$$\mathbf{G} = h \mathbf{b}_1 + k \mathbf{b}_2 + l \mathbf{b}_3 \quad (1.4)$$

that span the lattice space. For the reciprocal space we have:

$$e^{i\mathbf{GB}} = 1. \quad (1.5)$$

The unit cell within the reciprocal space is called Wigner-Seitz cell and is also referred to as first Brillouin zone, whose center is the Γ -point ($h = k = l = 0$). Between the vectors of the direct and the reciprocal space there are fixed relations and they are perpendicular to each other:

$$\mathbf{a}_i \cdot \mathbf{b}_j = 2\pi\delta_{ij}. \quad (1.6)$$

To describe periodic systems with quantum mechanical methods, one has to introduce periodic boundary conditions. These assume that the effective potential v_{eff} has to be the same in all cells that are given by \mathbf{B} :

$$v_{eff}(\mathbf{r}) = v_{eff}(\mathbf{r} + \mathbf{B}). \quad (1.7)$$

1.3 Atom Centered Basis and Peculiarities

Problem of plane waves for necessity of atom centered bases; Whenever there are atom centered basis sets the orbitals can overlap and due to this electrons are considered multiple times. This is called Basis Set Superposition Error (BSSE). One can apply Counterpoise corrections to get rid of this source of error. This is done here by calculating ghosted calculations with the system as a whole, the adsorbate alone, and the adsorbate with surface from ghost atoms. Then one applies a subtractive scheme to cancel out the effect of the orbital overlap. On the other hand one can use a huge basis set, that doesn't have this problem, which comes with a higher computational demand.

1.4 *Ab-initio* Molecular Dynamics

Microcanonical and Canonical ensemble, also called NVT and NVE. Difference between the two, N number of (?), V volume of the cell, T temperature and E energy; are kept constant. theory behind, calcuation of time propagation with Verlet algorithm, time steps chosen so that we don't miss the fastest processes, forces acting on atoms, Nosé Hoover thermostat.

Solve Newton's equations of motion, in principle $F = m \cdot a$ for force acting on each atom, classical ansatz.

$$-\frac{\partial V(\mathbf{R})}{\partial \mathbf{R}(t)} = M_A \frac{d^2 \mathbf{R}_A(t)}{dt^2} \quad (1.8)$$

1.5 Frequencies and Intensities

Normal Mode Analysis, diagonalization of the Hessian, eigenvalues are frequencies squared. While this is a good approximation for the high energy vibration, for example OD stretch vibrations, it becomes worse for lattice vibrations, which are way more delocalized. A characteristic of stationary points on the potential energy surface is, that the derivation with respect to all coordinates equals 0. For these points (minima and saddle points of first order) the Hessian matrix and their eigenvalues are of interest. The elements of this Hessian are the derivation of the potential with respect to coordinates:

$$H_{ij} = \left(\frac{\partial^2 V}{\partial Q_i \partial Q_j} \right)_{|Q_i=Q_j=0} = \left(\frac{1}{\sqrt{m_i m_j}} \frac{\partial^2 V}{\partial R_i \partial R_j} \right) \quad (1.9)$$

1 Theory und Methodology

Here, Q_i are mass weighted coordinates $Q_i = \sqrt{m_i}R_i$, with the mass m_i and the displacement from the equilibrium position R_i . Then the matrix problem for the Hessian \mathbf{H} has to be solved:

$$\stackrel{H}{=} \mathbf{A}_i = \lambda_i \mathbf{A}_i. \quad (1.10)$$

with the vectors of the normal modes A_i and λ_i being the squares of vibrational frequencies ω_i :

$$\omega_i = \sqrt{\lambda_i}. \quad (1.11)$$

One has to distinguish two physically relevant cases: all eigenvalues are positive ($\lambda_i \geq 0 \forall i$) so the structure is a minimum on the PES. This could be the educt and product of a reaction. The second relevant case is if there is only one negative eigenvalue, that gives according to equation 1.11 one imaginary frequency, respectively. This is in a mathematical sense a saddlepoint of first order and can be interpreted as a transition state.

dipole corrected NMA intensity can be calculated for IR spectra, not the same selection rules as for SFG but as a first approach should be feasible. Selection rules for SFG IR+Raman active, also the medium must not be version symmetric. **put the selection rules into the experimental details section?**

Tests with Born-effective charges: Intensities are also calculated via Born effective charges (BEC) where surface charges are determined and from that the intensities are obtained (dipole = charge*distance, $\mu^2 \propto I$).

Calculation of power spectra via velocity-velocity autocorrelation function from canonical MD trajectories. The vibrational density of states (VDOS) can be interpreted as the peaks of the spectrum. Through the motion of the atoms already some kind of quantum effects (not explicitly) are included.

$$VDOS(\omega) = \sum_{i=1}^N \int_{-\infty}^{+\infty} \langle v_i(t) \cdot v_i(0) \rangle e^{i\omega t} dt \quad (1.12)$$

1.6 Finding Transition States

One of the most prominent theories describing the transition state and the rate constants is Eyring theory of transition states **figure of reaction path?**. The most important approximations that are made are the following: all particles that reached the transition state will react towards the product. at the transition state geometry, the motion along the reaction coordinate can be separated from all other degrees of freedom and can be seen as a translation. The equation

1.7 From Density Functionals to Hybrids and Perturbation Theory

for the rate constant is described by

$$k(T) = \kappa \frac{k_B T}{h} e^{\Delta G^\ddagger(T)/(k_B T)}, \quad (1.13)$$

with the reaction rate constant k , Boltzmann's constant K_B , the temperature T , the difference of Gibb's free energy for the transition state and the educt ΔG^\ddagger and the transmission coefficient κ , that is a tunneling constant prefactor [tunneling corrections (seldomly applied in this work, not mention them here?)], give the reaction rate constant as a function of temperature and barrier height. For the latter one needs to find the energies of the transition state and the educt. The educt geometry can simply be obtained by geometry optimization as a minimum on the PES. To find the transition state geometry and henceforth the energy we used Nudged Elastic Band calculations (NEB), with Climbing Image, Reaction path is approximated as a series of associated images, which are connected via spring forces. These spring forces prevent the images from optimizing into the local minimum next to the transition state. First a regular NEB, then afterwards climbing image was done which gives better convergence. In this calculation the energetically highest image is "optimized" towards higher energies in the contrary direction of the gradient. For the point found by this scheme we checked whether this is a transition state via frequency analysis, since a TST of first order has to have one imaginary mode, that vibrates alongside the reaction path.

1.7 From Density Functionals to Hybrids and Perturbation Theory

In this work we also want to go beyond GGA (here the PBE functional), because it is known to underestimate reaction rates. Since we are interested in reaction kinetics it therefore is desirable to use more sophisticated methods to improve the rates. The first approach applied here is using hybrid functionals, where a fraction of exact exchange is mixed into the potential. Another ansatz is using Local Møller Plesset Perturbation Theory of 2nd order (LMP2) as implemented in crystal/crysor. These calculations are way more computationally demanding but offer better results on a higher level of theory.

1.8 Computational Details and Used Programs

Vasp4.x, 5.2 and version x (newer), crystal, cryscor, cp2k+i-pi, Turbomole
For all the vasp calculations for the (0001) surface the parameters from prior work in our workgroup was used, like vacuum gap and convergence criteria, because these were converged carefully by Dr. Jonas Wirth. Convergence was achieved when energies between 2 SCF steps

1 Theory und Methodology

was smaller than 10^{-5} eV.

For $(11\bar{2}0)$ surface parameters were adopted and used as well. Also here the convergence criterion for the energy of 2 SCF cycles was 10^{-5} eV.

For the other programs that were not used before for the calculation of alumina in our group the geometries from the vasp output were used as starting points and the usual convergence criteria of the programs were applied with some exception when convergence was hard to achieve.

1.9 Experimental Techniques

In this work several experimental techniques were used from our collaborating group at the FHI, that is why the basics of those methods are explained shortly.

1.9.1 Vibrational Sum Frequency Generation

energy scheme, uv and IR/visible Laser beam are overlapped spatially and in time, polarization is important, s and p polarized, selection rules: IR and Raman active, specificity for surface only in systems that are not inversion symmetric, good for studying surface systems, no bulk signals (both solid phase and gas phase) due to selection rules

1.9.2 Thermal Desorption Spectroscopy

Sample is heated with a defined temperature program, adsorbates are removed from surface according their binding energies and detected as a function of temperature. Sheds light on adsorption strength and probable reaction networks.

1.9.3 Molecular Beam Source vs. Pinhole Dosing

When doing the experiment the method of preparation seems crucial for the results, because these result in different surface situations. Our collaborators use the so called Molecular Beam Source but many other experimental groups use pinhole dosing. Here the idea behind these methods and the main differences shall be explained.

pinhole dosing: water is brought with a high partial pressure onto the surface. Problem here: in the gas phase and on the walls of the measuring chamber can be amounts of water that can influence the measurement. this leads to an equilibrium situation.

MBS: A medium, e.g. water is probed onto the surface at a very low pressure. Non-equilibrium situations are generated by the kinetic energy of the beam.

1.9.4 Low-Energy Electron Diffraction

Spectroscopical method for determining crystal structures in crystalline materials by an electron beam with an energy in the range from 20 to 200 eV. Diffracted electrons are observed as a pattern on the fluorescent screen. Structure can be derived from the geometry of this pattern. Lattice geometry can be seen. Problem is the high energy of the beam that can lead to damage in the sample.

Other methods as tunneling based methods do not work on isolating materials like alumina, so that it is simply not possible to measure STM. Others? Rasterkraft? ATM?

2 Water on $\alpha\text{-Al}_2\text{O}_3(11\bar{2}0)$

2.1 Surface Model

The structure of α -alumina is well known for several years. It crystallizes in the hexagonal cell, that means $a=b\neq c$, with an angle of 60° between a and b .

To obtain the clean surface we cut a 2×2 supercell from bulk structure. The cell vectors were used from the bulk structure and a vacuum gap in z-direction (perpendicular to the surface) was introduced.

The unit cell consists of 5 atomic layers in z direction ($\text{O}-\text{O}_2-\text{Al}_4-\text{O}_2-\text{O}$), our supercell has 10, where the lowest 5 were fixed to the bulk value to mimic the surface situation. For the phonon calculations more layers were considered (up to 25 layers), here also for each slab size the lowest 5 layers were kept fixed, respectively (see chapter 2.4.2).

k -point tests were done for 5 different grid sizes from $1 \times 1 \times 1$ to $5 \times 5 \times 1$. In contrast to the even grid sizes, the odd ones contain the Γ -point and therefore are favorable. It was shown that the $3 \times 3 \times 1$ grid is already converged with respect to the energy of the clean surface, see fig. 2.1.

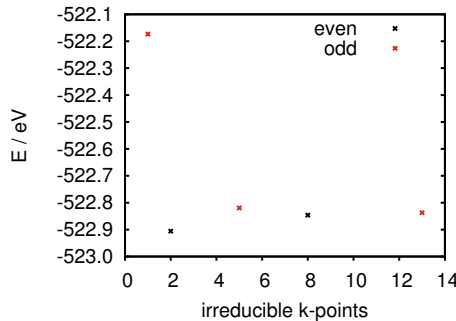


Figure 2.1: Sampling of the k -points, shown is the energy of the super cell with respect to the number of irreducible k -points. The even values correspond to the $2 \times 2 \times 1$ (2 irreducibles) and $4 \times 4 \times 1$ (8 irr.), whereas the odd, that contain the Γ -point, are described by $1 \times 1 \times 1$ (1 irr.), $3 \times 3 \times 1$ (5 irr.) and $5 \times 5 \times 1$ (13 irr.).

Starting from this supercell approach there are 16 CUS Al-atoms (cordinatively unsaturated sites), these have less bonds than the aluminum atoms in the bulk structure since the surface

2 Water on $\alpha\text{-Al}_2\text{O}_3(11\bar{2}0)$

layers has to be depleted. These atoms are very interesting for adsorbate molecules/atoms, because these atoms are electron rich and can be addressed for adsorption. If these 16 atoms are covered with adsorbates, here water, we get the system with 1 mono layer (ML). But one has to keep in mind the difference between these 16 surface atoms and the number of potential adsorbates: one monolayer is not built by 16 adsorbates since not all 16 CUS positions can be covered, but only 12, as is shown later (bridging water adsorption).

As is shown with different colors in figure 2.2 (b) and (c), the system consists of different types of CUS Al atoms with different coordination neighborhood and 2 different types of oxygen atoms, 2-fold and 3-fold coordinated. The Alumina atoms have the same number of oxygen neighbor atoms but differ slightly in the arrangement of their neighbors and the distance in the relaxed structure, but the oxygen atoms in fact differ by the number of neighbors. In this work, the black spheres denote the CUSb atoms, the grey ones depict the CUSA, the two-fold coordinated oxygen atoms ($O-\mu_2$) are shown in yellow and the three-fold coordinated ($O-\mu_3$) in red. Atoms of the underlying layers are illustrated in pale colors, light grey for alumina and pale red for oxygen.

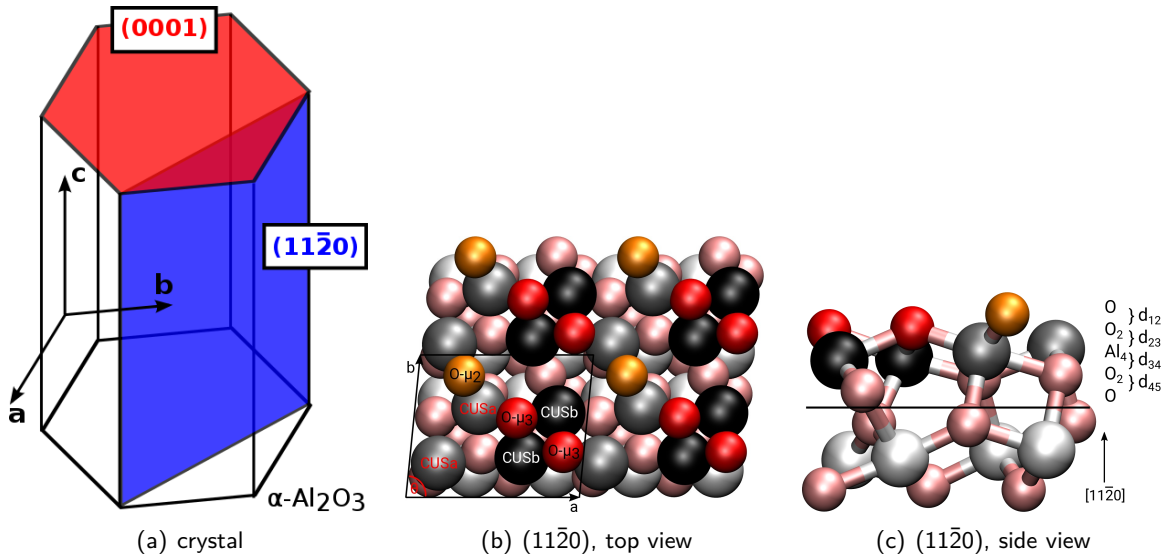


Figure 2.2: The crystal cut of $\alpha\text{-Al}_2\text{O}_3$, (a) schematic compared to the (0001) surface, (b) a top view of the unit cell with the nomenclature of the surface atoms and (c) as a side view showing the different atomic layers.

2.2 Structure Search

First a low coverage regime was investigated: 1 water molecule per 2×2 supercell, which equals a coverage of 1/12. It was put on different positions on the surface and let relax. We found 1 molecular minimum and several dissociated species including both CUS and oxygen types, for adsorption energy and Gibb's free energy results see table 2.1. There is also one metastable molecular species that seems more stable than the found molecular minimum, but since there is one imaginary mode displaying the movement of the proton towards the dissociated species this cannot be classified as a stable minimum. The adsorption energy is defined by equation 2.1 as the energy of the adsorbed system compared to the energies of the clean surface and the isolated water molecule:

$$E_{\text{ads}} = E_{\text{ads. species}} - (E_{\text{free water molecule}} + E_{\text{surface}}). \quad (2.1)$$

The nomenclature for the adsorption sites that is used in the following gives at first the type of Al site where the OH-residue (OH^-) is adsorbed and at second place the oxygen type where the H(/H⁺) is adsorbed (OH-site||H-site). The notation with the / that will occur later denotes greater distances between the residues. The molecular minimum is substantially less stable

Table 2.1: change text! Adsorption energies as calculated from equation 2.1 for molecular and (singly) dissociated water on $\alpha\text{-Al}_2\text{O}_3(11\bar{2}0)$ according to periodic PBE+D2 calculations. Also the corresponding adsorption free energies G_{ads} at 130, 300 and 400 K defined analogously are also given. The three most stable configurations are in bold. All energies are given in eV.

Adsorbed Species		E_{ads}	$G_{\text{ads}, 130 \text{ K}}$	$G_{\text{ads}, 300 \text{ K}}$	$G_{\text{ads}, 400 \text{ K}}$
molecular	CUSb	-1.78	-1.60	-1.51	-1.46
dissociated	inter-CUSa O-μ_2	-2.50	-2.27	-2.16	-2.09
	inter-CUSa O- μ_3	-1.67	-1.44	-1.33	-1.27
	CUSb O-μ_2	-2.28	-2.12	-2.03	-1.97
	CUSb O- μ_3	-1.19	-1.05	-0.98	-0.95
	inter-CUSb O-μ_2	-2.09	-1.88	-1.80	-1.76
	inter-CUSb O- μ_3	-1.89	-1.71	-1.63	-1.58

than the dissociated species. On the contrary, the dissociated water is very stable, also in comparison with the more stable surface cuts (0001) and (1102) that were investigated before in our group by Dr. Jonas Wirth [?, ?]. Dissociated species, where the proton is located at a two-fold coordinated surface oxygen is far more stable than the corresponding systems where the three-fold coordinated is occupied, since the higher negative charge and the higher basicity of such a two-folded oxygen atom in comparison with the more saturated three-fold coordinated

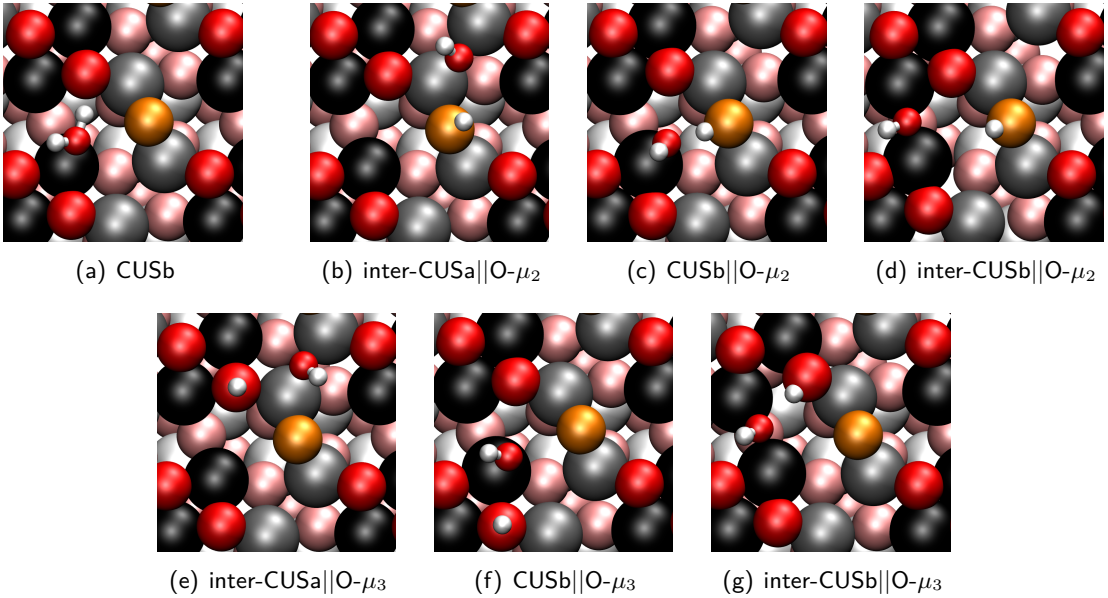


Figure 2.3: change text! Adsorption geometries for molecular (a) and (six) dissociated water molecules ((b)-(g)) are shown, as obtained by periodic PBE+D2. The most favorable molecularly and dissociatively adsorbed configurations are shown. This means that we show nearest neighbor structures only (see text). The color code is the same as in Figure 2.2(b) and (c), CUSa grey, CUSb black, O- μ_2 yellow and O- μ_3 red; Hydrogen is displayed in white, subsurface layers are in pale colors.

O- μ_3 oxygen atom. Also the adsorption of OH at an inter-CUSA site is more favorable than at a CUSb site, because the former corresponds to a site where in the bulk system another oxygen atom would be situated, which is not the case for the CUSb position.

Dissociated species in direct neighborhood as shown in table 2.1 and figure 2.3 are more stable than those where the proton and the OH residue are further apart (see table 2.2), because the OH residue has a stabilizing effect on the H. In the table one can see, that the inter-CUSb \parallel O- μ_3'' -species is more stable than the species inter-CUSb \parallel O- μ_3' . This is due to the fact, that the periodic conditions lead to the decrease of the distance between OH groups again, so that between 3 neighboring OH groups in the O- μ_3' system the distances are 0.68 and 0.77 nm, whereas in the O- μ_3'' system the distances are 0.93 and 0.62 nm, where the latter one is closer by, so there is more stabilization. For examples of further diffusion reactions, see chapter 2.3.

Also systems with a higher water coverage were considered, tests for 2 water molecules, 4 inter-CUSA \parallel O- μ_2 and a fully covered supercell, for these systems also normal mode analyses were done to get vibrational spectra, see also chapter 2.4.2.

2.3 Reactions and Microkinetic Model

Table 2.2: Comparison of next neighbor dissociated species and species where OH and H are further apart.

Adsorbed Species	$E_{\text{ads}}[\text{eV}]$
inter-CUSa O- μ_3	-1.67
inter-CUSa O- μ'_3	-1.42
inter-CUSb O- μ_3	-1.89
inter-CUSb O- μ'_3	-1.16
inter-CUSb O- μ''_3	-1.22

The stability of those species with higher water coverage is defined as

$$E_{\text{ads}} = E_{\text{ads. species}} - (E_{\text{free water molecule}} \times n + E_{\text{surface}}), \quad (2.2)$$

with n being the number of water molecules adsorbed on the surface. In table 2.3, the adsorption energies are given. Comparing these results for the higher coverages to results with only

Table 2.3: Adsorption energies in eV for higher water coverages. For comparison in the third column the added energies for singly adsorbed water are shown.

Adsorbed Species	E_{ads}	isolated species
CUSb(mol)+CUSb O- μ_2	-4.57	-4.06
inter-CUSa O- μ_2 +CUSb O- μ_2	-4.77	-4.78
2inter-CUSa O- μ_2	-4.84	-5.0
4inter-CUSa O- μ_2	-9.55	-10.0
12H ₂ O	-23.39	unclear..

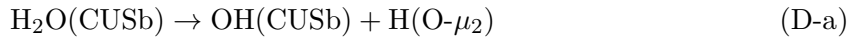
one adsorbate, just by adding the adsorption energy one can see the following (see also column 3 in table 2.3): For all systems the added energy of the singly adsorbed species is more stable than the doubly adsorbed water systems. Instead of stabilizing the whole system, they are destabilized by the adsorption neighborhood, even in structures that contain hydrogen bonds.

2.3 Reactions and Microkinetic Model

Based on the minimum structures one has to identify reaction pathways to fully understand the reactivity of a system, so we utilize the NEB method including Climbing Image to search for transition states between the minima. We examined 3 different types of reactions: dissociation from the molecular minimum, as well as OH-diffusion and H-diffusion. The dissociation reactions are named D, diffusion reaction with Df in table 2.4 and figures 2.4 and 2.5. In reference 11-20paper only some reactions were introduced, additional reactions paths are given.

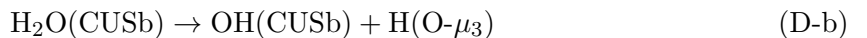
2 Water on $\alpha\text{-Al}_2\text{O}_3(11\bar{2}0)$

We investigated 5 different dissociation reactions. The two that were already shown in the publication 11-20paper are the reactions from CUSb to the two fold coordinated oxygen (D-a) and one to the three fold coordinated O (D-b). One additional dissociation starts from the metastable inter-CUSA molecular structure that is, as was shown before, no minimum structure end goes to the most stable species inter-CUSA||O- μ_2 (D-c). 2 dissociation reactions converged but showed a two step process and are therefore not interesting in the first place (these reactions are CUSb→inter-CUSA||O- μ_2 and CUSb→inter-CUSb||O- μ_2 put them into appendix?). As can be seen from chapter 2.2 (table 2.1), the molecular minimum CUSb is very low in stability compared to the dissociated minima. The first reaction, D-a leads from the molecular minimum at CUSb to the two-fold coordinated CUSb||O- μ_2 .

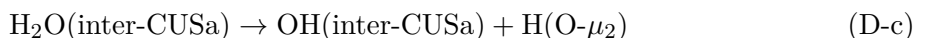


The barrier is very low, about 0.002 eV as one can see from table 2.4 and figure 2.4(a), hence the reaction rate constant is very high, in the range of 10^{12} s^{-1} . This low barrier might be due to underestimation of barrier heights with the used functional PBE.

For the other dissociation reaction D-b from CUSb to CUSb||O- μ_3 , there is no barrier found at all, the reaction pathway shows simply an upgoing path in energy without any barrier, since the molecular minimum is by 0.15 eV more stable than the dissociated structure on CUSb||O- μ_3 .



A further dissociation D-c from the metastable inter-CUSA species also shows no barrier, probably because the educt is no real minimum.



optimizations with the intact water molecule placed over CUSb and inter-CUSA lead to a intermittent structure of a molecularly adsorbed species which dissociated later for both cases. The OD diffusion reaction Df-OH-a moves from CUSb||O- μ_2 to the inter-CUSb position, which is relatively fast for OD diffusion reactions compared to the reactions at other alumina surfaces.



In this special reaction, the OH residue diffuses from an on top CUS position into a gap between two CUSb atoms, so that there is not much interaction with neighboring surface oxygen atoms and other CUS atoms nearby during the diffusion. In contrast to that the reaction Df-OH-b is

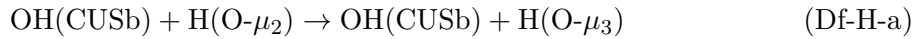
2.3 Reactions and Microkinetic Model

much slower. It is a diffusion from CUSb to inter-CUSA with the hydrogen residue staying at an O- μ_2 position. This barrier is with 1.07 eV higher.



This is more in the range of OH diffusion reactions for other alumina surfaces (compare to doctoral thesis of Dr. Jonas Wirht, UP 2016??), where the rates for the (0001) surface is 10^xs^{-1} and for the (1̄102) surface the corresponding process is around 10^ys^{-1} . **check these numbers in Jonas' thesis!**

A bigger variety can be achieved when looking at H diffusion reactions. The different types of surface oxygen atoms and also the distances between OH and H residue make differences in the observed reactions. As seen before, the hydrogen is preferably found on the two fold coordinated oxygen atom, but the reaction to a neighboring three fold coordinated oxygen is very plausible and opens the gate to structures with greater proximity. The reaction takes place with the OH residue being on a CUSb site:



barrier height and rate at 300 K... A similar reaction starting from the most stable inter-CUSA||O- μ_2



barrier, rate constant at 300 K.. The following reactions deliver structures with increased distance between OH and H residues. As mentioned before, the nomenclature uses for these structures primes (\prime) to display the distance. This reaction starts with OH sitting on inter-CUSb and the hydrogen being adsorbed on an O- $\mu_2\prime$ position, diffusing further away to O- μ_3'' , which is less in stability:



this reaction is not ready yet; barrier and rate constant. The last reaction leads to the position where OH and H have the greatest possible distance with the applied periodic boundary conditions:



2 Water on $\alpha\text{-Al}_2\text{O}_3(11\bar{2}0)$

rate constant and barrier.

add here the part with the diffusion part for the proton from next neighbor to highest distance possible!

Table 2.4: CHANGE THIS TABLE COMPLETELY!! Reaction rates for selected reaction paths examined. $\Delta E = E(\text{product}) - E(\text{educt})$, $\Delta E^\ddagger = E^\ddagger - E(\text{educt})$, respectively for the free energy, G , obtained from PBE+D2 calculations. k is the rate constant from eq. (1.13). Thermodynamic quantities and rates are given for $T = 300$ K. “n.f.” indicates “not found”. The reactions are either water dissociation (D), OH diffusion (Df-OH) or H diffusion (Df-H).

Reaction Type		ΔE (eV)	$\Delta G_{300\text{ K}}$ (eV)	ΔE^\ddagger (eV)	$\Delta G_{300\text{ K}}^\ddagger$ (eV)	$k_{300\text{ K}}(\text{s}^{-1})$
H_2O dissociation	D-I	-0.50	-0.52	0.01	0.002	5.76×10^{12}
	D-II	0.59	0.53	n.f.	n.f.	n.f.
OH diffusion	Df-OH-III	0.19	0.22	0.35	0.39	1.88×10^6
	Df-OH-IV	-0.21	-0.13	1.07	1.10	2.41×10^{-6}
H diffusion	Df-H-V	1.08	1.04	1.65	1.49	4.90×10^{-13}
	Df-H-VI	-0.06	-0.07	1.05	0.94	1.05×10^{-3}

Also tried to study the adsorption/desorption process but didn't find a barrier, energy profile behaves smoothly from water molecule above the surface to the adsorbed water system.

Problem of GGA underestimating barriers is well known. Optimizing structure with HSE06 is nearly impossible due to high cost and doing single point calculations on the PBE transition state is not very accurate and doesn't deliver better results. (at least for crystal calculations... so don't bring it her?)

For the OH diffusion we find that a special case of CUSb to inter-CUSb diffusion is favored, because the distance that has to be bridged is very small; but real CUS to CUS diffusion like the one from CUSb to inter-CUSA is very slow.

TEST?? What doesn't work is the molecular diffusion from CUSb to CUSb, the molecular minimum is not stable enough, during the path, dissociation would occur? Or it would have to be a two step reaction from CUSb to inter-CUSb what does not exist and then further to CUSb..

Proton diffusion reactions are way more variable giving reaction rates at 300 K ranging from 10^{-x} to 10^{+y}s^{-1} . The barriers and therefore also rate constants for H-diffusion cover a wider range depending on the distance between OH and H and of course more importantly on the fact between which type of $\text{O}\mu_2$ the proton is diffusing.

Also reactions leading to a not next-neighbored situation, increasing the distance between OH and H are also not favorable since geometries with the residues further apart are energetically

less stable.

what about backreactions?

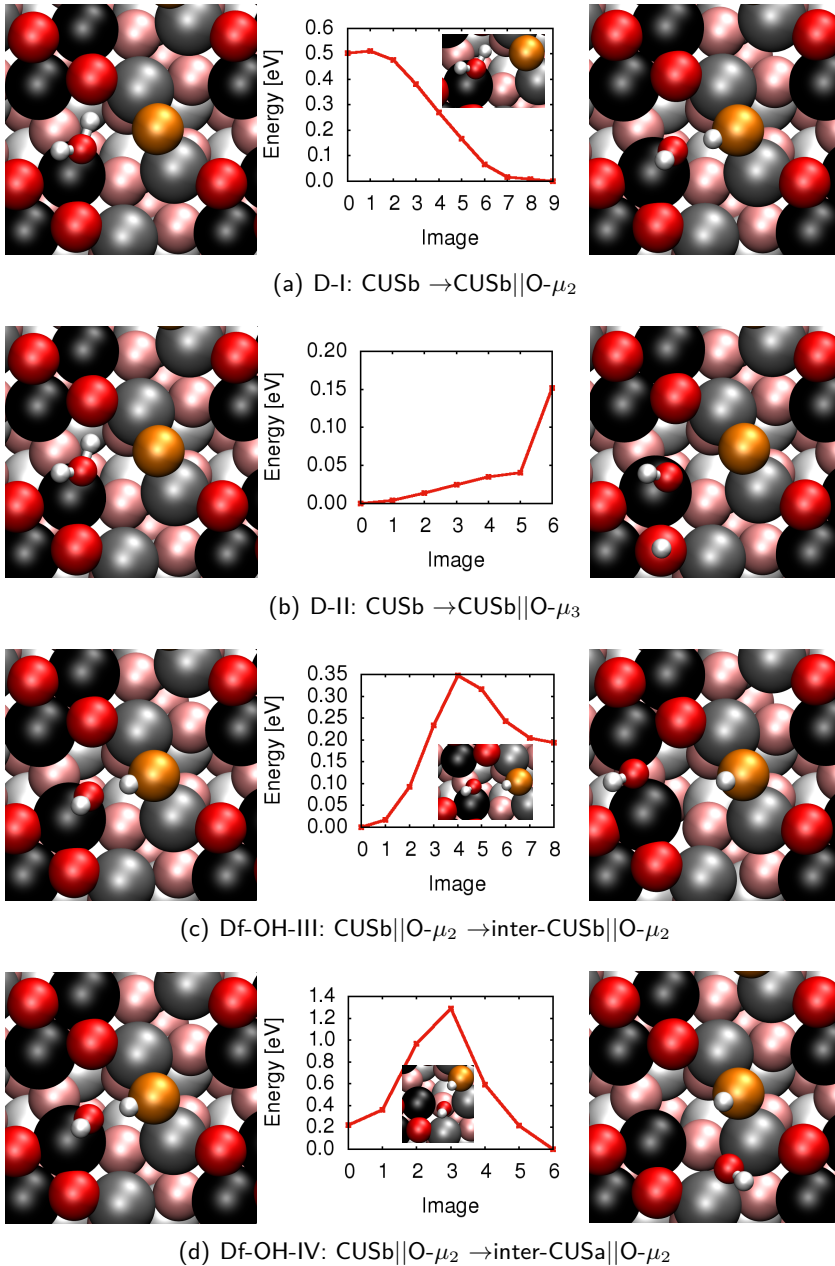


Figure 2.4: PBE+D2 minimum energy paths with transition states (inlay; if available), and both educt (left) and product (right) states for D-I, D-II, Df-OH-III and Df-OH-IV reactions, respectively. The color code is as explained above.

2 Water on $\alpha\text{-Al}_2\text{O}_3(11\bar{2}0)$

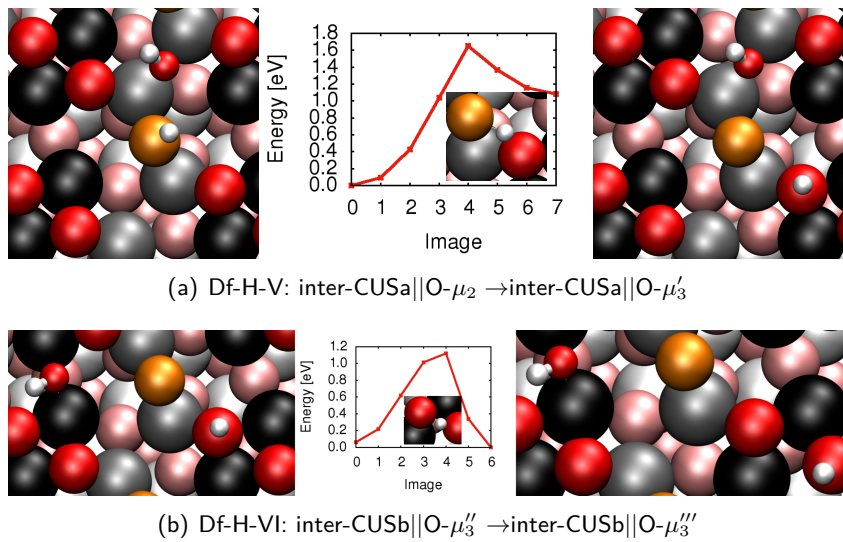


Figure 2.5: PBE+D2 minimum energy paths with transition states, and both educt and product states for Df-H-V and Df-H-VI reactions, respectively. The color code is as explained above.

add newly started iCb2'-iCb3pp and the path from iCb3 over iCb2' over iCb3pp to iCb3ppp as an example for proton diffusion pathways.

2.4 Vibrational Frequencies / Spectroscopic Properties

A great source of knowledge about chemical systems comes from vibrational spectroscopy, so we were interested in frequencies of the systems, since the frequencies of these vibrations give us hints about the chemical environment as hydrogen bonds and other atoms nearby that bond to each other. These vibrational frequencies were calculated for the surface system with OH and also with OD. Our experimental partners from FHI use deuterated water (D_2O) instead of H_2O because the chemical reactivity is the same but the spectroscopic properties are better with their applied Laser system. The experimental SFG spectra (Sum Frequency Generation) for the OD range of the low coverage regime for two different coverages are shown in fig. 2.6. Of course, the frequencies for a deuterated system are different from OH, but the different isotope names can be calculated easily within vasp by changing the mass. To calculate the modes we mainly applied two methods: Normal mode analyses (see section 2.4.1) and power spectra from velocity-velocity autocorrelation function (section 2.4.1).

The intensities are implicitly in the power spectra and for the normal mode analyses we follow 2 different approaches, dipole corrections and Born effective charges. But mostly we are interested in the position of the modes and not in the relative intensities, because these are not too

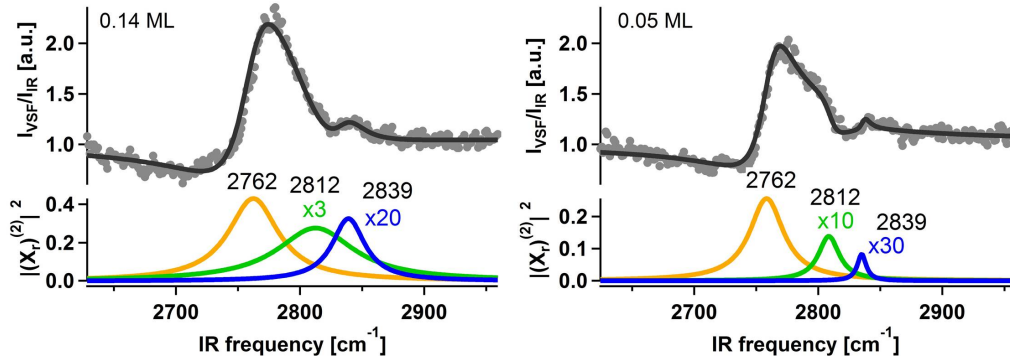


Figure 2.6: Experimental SFG results including fit.

reliable.

In another part, the modes for higher coverage systems are also examined.

TODO: Listed all frequencies for all possible next neighboring structures are shown but in comparison with the experiment, we only focus on the 3 most stable adsorbate structures, since only those are expected to be seen in experiment.

2.4.1 OH/OD Vibrations

Normal Mode Analysis

The classical modes calculated with a normal mode analysis are dependent on the mass and the spring constant of the bond. We assumed that the OH/OD stretching modes for the 3 most stable structures (of course for all others as well in order to check whether a structure is a minimum) would contribute to the spectrum the most. Following this approach we expect 6 modes (2 for each, one of the adsorbed OH group and one for the surface group). We expect 6 frequencies. when evaluating those values one can see that one is out of the experimental range (strongly hydrogen bonded species, wave number is shifted to low $\tilde{\nu}$ and some of the others are except for numerical differences the same, so there should be only 3 bands visible. Very good agreement with the experimental modes. The numbers itself do not compare too good, but the relative modes are in really good agreement.

Comparison of different slab sizes.

Comparison of intensities with dipole corrections and Born effective charges.

Velocity-Velocity Autocorrelation Function

Extract vel vel autocorrelation function from MD at 300 K (and also 400 K?) from most stable structures (inter-CUSa||O- μ_2 , CUSb||O- μ_2 and inter-CUSb||O- μ_2), with Fourier transforma-

2 Water on $\alpha\text{-Al}_2\text{O}_3(11\bar{2}0)$

tion converted to VDOS spectrum. It also is possible to separate Modes from water layers from bulk phonons. Not really important if you don't use hydroxylated surface with a higher water coverage?

2.4.2 Lattice Vibrations

For the phonons as a first test the same normal modes analyses were checked to get a first impression into how the spectra can look like. But for a better description we need to consider more layers of the bulk in order to get more reliable results. From an experimental point of view it is suggested that SFG spectra can give insight into **x** layers of the bulk. Therefore we did calculations for the most stable adsorption geometries for more layered systems, going up to $6*5=30$ layers, both for the naked surface and for the covered surface, here we used again optimized geometries of the most stable structures. These results are also shown with intensities calculated from dipole corrected normal mode analyses.

2.5 Desorption Process

calculation with NEB didn't lead to anything, there is no barrier visible

`/und/sophia/bigger-cell_newcrystalcut/2x2cell/2layers/gasphase-physisorbed`

As mentioned before the experimentalists measure TPD in order to understand the adsorption strength and possible exchange reactions. We tried to simulate the desorption process using the following scheme: take the water in the gas phase + the naked surface as the standard. In the thermal equilibrium, the water should be equally distributed to Boltzman's distribution in the most stable structures. From this situation the water can recombine to the molecularly adsorbed water. The recombined water then can desorb to the gas phase. Since the spectrum is measured in ultra high vacuum it can be assumed that all the water that has left the surface will not return to the system, because it is dragged out of the equilibrium by the vacuum pumps. Applying the reaction rates of the corresponding reactions in a kinetic Monte Carlo approach leads to **REDO THESE CALCULATIONS**.

3 Water on $\alpha\text{-Al}_2\text{O}_3(0001)$

The most stable surface site under UHV conditions, subject of several studies so far.

3.1 Surface Model

Crystal structure of $\alpha\text{-Al}_2\text{O}_3$ with surface cuts (0001) and (11 $\bar{2}$ 0) in comparison. We applied here a 2×2 supercell with, as before, vectors as in the bulk (did Jonas optimize them?) Al terminated surface, only one type of CUS, all oxygen atoms are 3-fold coordinated, topography is not as complicated as for the higher indexed surface. x layers, y fixed.

1 Water molecule per 2×2 supercell was already studied by Dr. Jonas Wirth, but in order to understand the chemistry, one has to know how water reacts in this system. There is one molecular minimum on top of a CUS atom and mainly 3 dissociated states, the next neighboring 1-2 dissociated state, the 1-4 dissociated structure with the Hydrogen atom being one position further and the 1-4' that is the configuration with the greatest distance that is possible for this slab size. The 1-2 diss is the most stable one and the 1-4' is the least stable one. For the molecular and the 1-4 diss, the stability is, depending on the method, but lies between the previously mentioned ones, for some methods PW91+D2(?) it is the same adsorption energy (the value is calculated as for the (11 $\bar{2}$ 0)), or for some methods and basis sets tested with crystal the one or the other is more stable.

Of course there are reactions linking these minima, dissociation, OH- and H-diffusion were studied, as well as rotation of a OH group and molecular water diffusion from CUS to CUS. The latter two do not play a crucial role in this work.

3.2 AIMD for Dissociation Process

Hass et. al. discussed the idea whether water will adsorb molecularly first and then dissociate or if direct dissociation upon adsorption is possible. To tackle this question for the experimental technique of the molecular beam source, we apply both microcanonical and canonical *ab-initio* MD to simulate the water molecules in the beam approaching the surface. We start in the low coverage limit by letting one single, rigid molecule approach the 2×2 supercell.

3 Water on $\alpha\text{-Al}_2\text{O}_3(0001)$

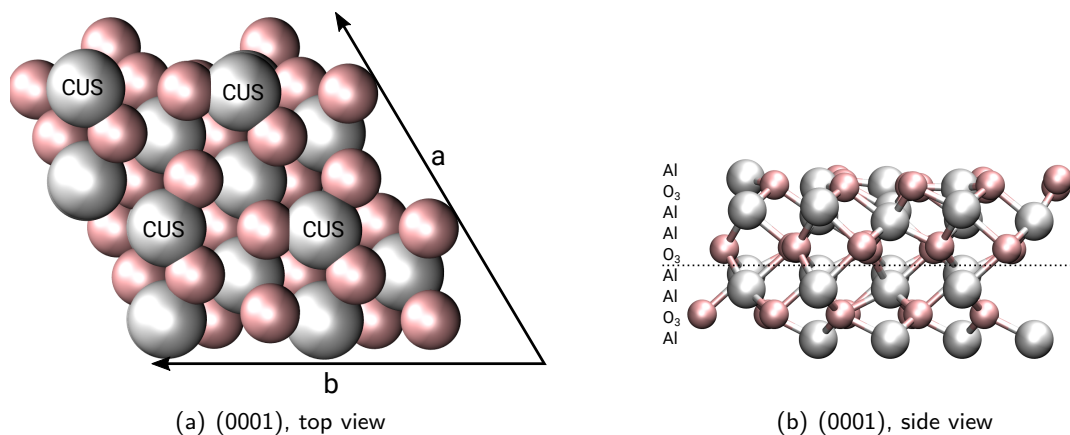


Figure 3.1: Surface model (0001).

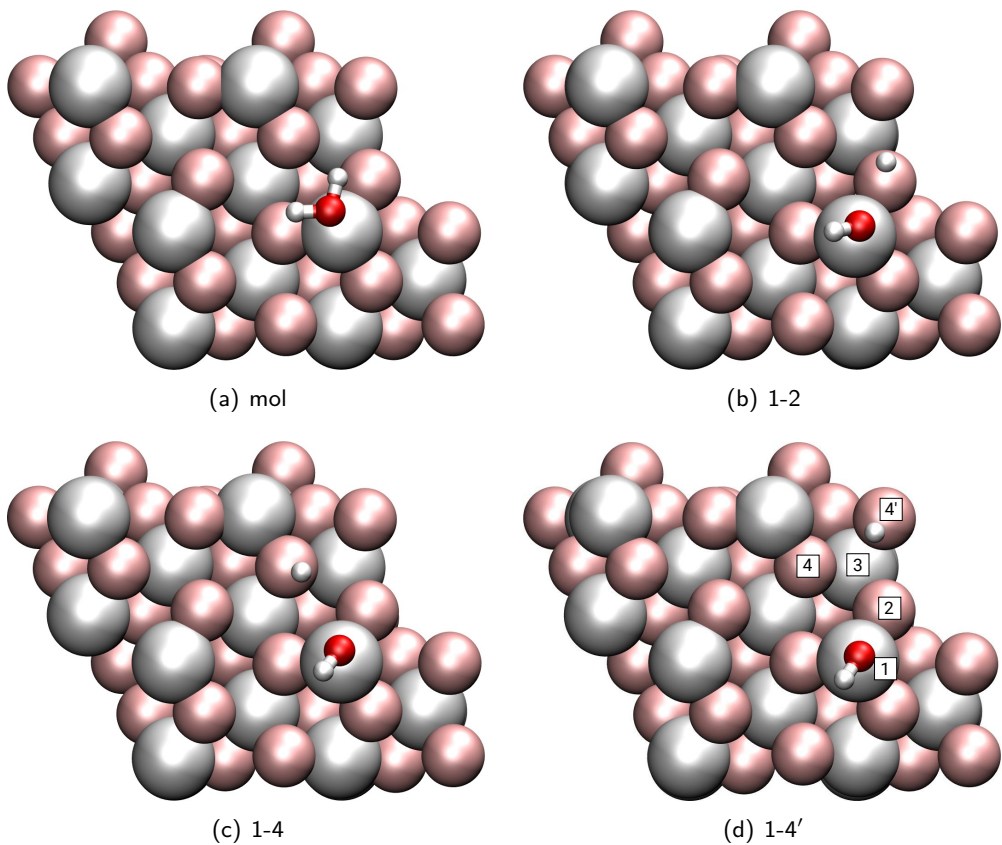


Figure 3.2: Adsorption geometries molecular and 3 dissociated species.

We later on continue with different approaches to more realistic beams and to more realistic surface situations. In the beam regime we probe water clusters, namely pre-optimized $(\text{H}_2\text{O})_2$

3.2 AIMD for Dissociation Process

and $(\text{H}_2\text{O})_4$ cluster, which are shot onto the surface. Another improvement to the beam lies in having the molecule either vibrationally and/or rotationally excited. These excitations were chosen from a normal mode analysis and the resulting stretch and bending modes.

For improving the surface we first use a preequilibrated surface at 300 K, but also go to a surface situation in which already one water molecule is adsorbed. To pay attention to the equilibrium situation we considered a molecular preadsorbed water molecule, the most stable 1-2 dissociated state as well as the 1-4 dissociated structure.

We could show that water can both dissociate upon direct contact with the surface and also dissociate after being adsorbed molecularly first and then after a time have enough energy to dissociate. This is mostly to the 1-2 dissociated state but also 1-4 and more surprisingly 1-4'. It seems that the rotation of the water molecule before hitting the surface is crucial for direct dissociation. This energy can also be delivered by the heated surface, it has more energy in form of vibration, in this case prolongation of the respective OH bond and can therefore lead to dissociation. On the other hand hitting the surface directly on top of a CUS atoms was shown to lead mainly to reflection of the molecule, because the energy of the incoming molecule could not be absorbed by the surface.

Trajectories with the vibrationally excited modes led to statistically higher levels of dissociation. Also temperature effects of the thermalized trajectories (canonical MD) seem to have a positive influence on the dissociation.

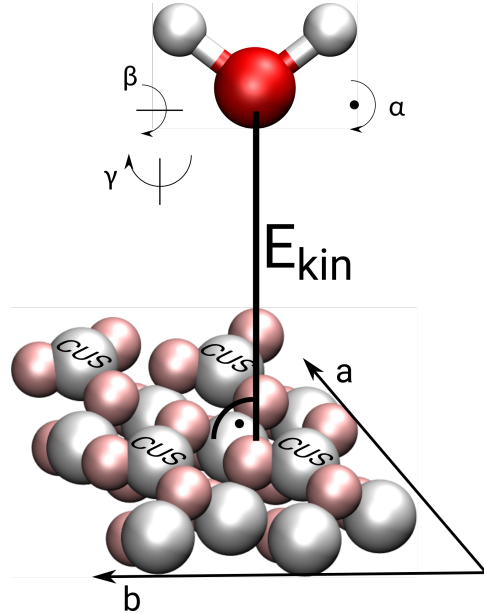


Figure 3.3: Sketch for initial parameters of the trajectories.

3 Water on $\alpha\text{-Al}_2\text{O}_3(0001)$

3.2.1 Microcanonical

Cluster

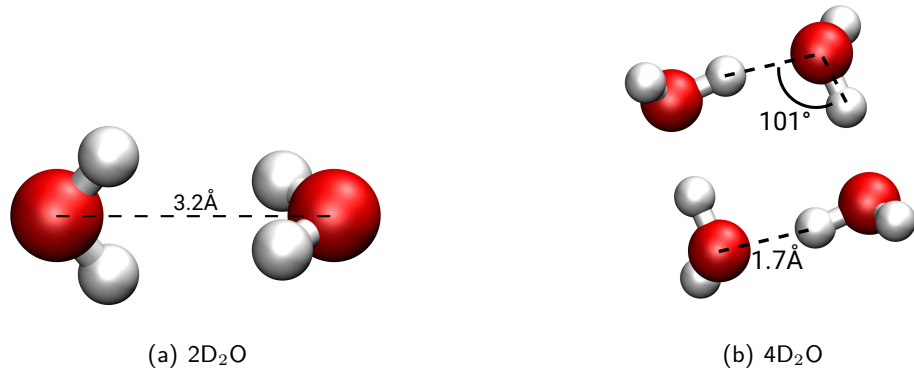


Figure 3.4: Clusters for simulation of effects of higher coverages.

Ppreadsorbed Surface

Rotationally and vibrationally preexcited Water

3.2.2 Canonical

3.3 Improvement of Reaction Rates

For a model reaction we try to improve the reaction rate with different new methods. This reaction is a H-diffusion reaction on the (0001) surface studied before in our group, the Df-H-4-2 reaction, that moves a proton in the 1-4 position to the OH residue to the 1-2 dissociated state. The rates were before calcualted with PBE+D2/3? and Nudged Elastic Band. An approach were singlepoint calculations were done for the minima and the transition state was also done. For this process also a 1-D potential energy surface was calculated and then the Schrödinger equation was solved to obtain the wave function and see the localization/delocalization of the reaction pathway.

Now we want to expand these methods to the following 3/4/don't know? First we want to calculate the adsorption energies and the barrier within a atom centered orbital method with the hybrid functional B3LYP and also go beyond density functional theory and go to perturbation theory (LMP2).

Apart from that, we study this reaction with the help of Path Integral Molecular Dynamics, where the system is represented as a couple of beads that are connected and henceforth act as a more delocalized particle which can contribute to quantum effects, proton tunneling.

As a last approach, we want to apply other higher level methods in an embedded approach. We cut a cluster from the surface situation and embed this cluster in a field of point charges. By doing this we can calculate the cluster with a better method, let's say B3LYP, CCSD or MP2 and then apply a subtractional scheme to get to corrected adsorption energies that can then be used to improve the rates with Eyring's equation for transtition states.

3.3.1 MP2 and B3LYP

Going beyond pure density functionals and also beyond DFT has been too costly for a long time, simply not applicable for surface adsorbat system that large and electron rich. In the crystal/cryscor code one uses atom centered bases instead of plane waves and so large scale systems can also be computed. We first optimized our parameters with HF calculations and then did calculations with PBE similar to prior plane wave based calculations.

We found out, that BSSE takes a big part, but corrections are not easily applied because the ghosted calculations needed for that do not converge for all the structures with a bigger OH-H distance. Instead we have to use bigger basis sets containing diffuse functions in order to handle the BSSE. Such a self designed basis set by our cooperation partner Dr. Denis Usvyat (HU Berlin, group of Martin Schütz) was used here. With this basis set we did the PBE calculations again (?) and the B3LYP as well as the MP2 calculations. First we compared the differences in adsorption energies. We furthermore compared the vibrational frequencies from B3LYP with

3 Water on $\alpha\text{-Al}_2\text{O}_3(0001)$

the ones from VASP/PBE to see a methodological effect.

We also reoptimized the transition state for the Df-H-4-2 reaction.

Not sure if this will come into the diss? No real results obtained..?

3.3.2 PIMD

Instead of examining reactions with a defined reaction pathway as with NEB, we apply the path integral MD to propagate the 1-4 dissociated state in the hope to watch the reaction and to extract from that a time for the reaction (*? it is not really a rate*). But unluckily, no reaction occurred in the given propagation time, so that one only can see the delocalization of the proton. At a given temperature of 300 K the proton only moves a little, far away from any reactive trajectory.

A huge problem was the unit cell: when all atoms or only a few atoms were allowed to move during the trajectory, the whole cell drifted away, as if the periodic boundary conditions would not apply. When fixing all the atoms except for the proton that diffuses it was fine.

cell optimizations were tried, but didn't work as planned; fixing only the rim lead to other atom's movement, maybe one can free the OH group and the Al atom on which the H sits?

We used also PBE but without dispersion corrections and for the trajectories at 300 K we applied the Nosé Hoover thermostat.

3.3.3 QM/QM Embedding Scheme

In order to recalculate adsorption energies and reaction rate constants with a higher level method we tried to apply the mechanical embedding scheme developed in the Sauer group from HU Berlin. One uses a subtractive scheme to correct energies, after calculating the complete system with the low level method (here PBE), the interesting part, namely the cluster, with both the low level method and the high level method (B3LYP, MP2 or CCSD). The high-level:low-level corrected energy is then calculated by the following equation: *equation* First of all, a reasonable cluster has to be chosen, which is difficult since the 1-4' needs a big cluster to be considered. We chose then the Al_8O_{12} -cluster used in unpublished work from the same group. This cluster was used for tests but when it came to embedding, the Turbomole package failed to compute the embedded system, because hexagonal cells were not yet implemented into the code.

Summary

We made great progress in understanding the $(11\bar{2}0)$ surface of $\alpha\text{-Al}_2\text{O}_3$ in contact with water in the low coverage regime.

The dissociation process of water on (0001) surface was studied.

Several methods were tested to improve reaction rates.

Acknowledgment

I want to thank my doctoral father Prof. Dr. Saalfrank, for giving me the scientific opportunity to research on surface systems and all the valuable discussions and advices. Also I am deeply grateful to my supervisor Dr. Jonas Wirth who gave me support during my time starting as a Bachelor's student, during my Master's thesis and also through the beginning of my PhD, PD Dr. Tillmann Klamroth for discussions about programming and theoretical questions that arose during the work, Dr. Radosław Włodarczyk for his endless knowledge with vasp and programming in general, Giacomo Melani (soon to be Dr.) for his advice and his help, and also the discussions about our teaching duties in mathematics and the whole workgroup for all the valuable discussions and the help. Also for the great atmosphere, that was some times productive and some times also just relaxing and felt very comfortable, here especially Clemens Rietze, Robert Scholz, Gereon Floss, and Steven Lindner. Also I want to thank my second supervisor Beate Paulus for discussion and help beyond research topics. Great acknowledgement to my experimental cooperation partners from FHI, Yanhua Yue, Dr. Harald Kirsch and Dr. Kramer R. Campen for the great work and publications we did together. Thanks to Dr. Denis Usvyat for all his patience and knowledge and valuable discussions about crystal/crysccor and his help. Maristella Alessio from Sauer group (HU Berlin) for help with Turbomole and setting the mechanical embedding calculations, that unluckily did not work for the applied cluster. Ji Chen and Wei Fang from Michaelides group from UCL London for their help with cp2k and i-Pi, necessary for the PIMD calculations. Last I want to thank Dr. Jean Christophe Tremblay who brought me to theoretical chemistry by bringing my attention to this field of science. Christiane Wunderlich who was my school teacher in chemistry, without whom I would not have studied chemistry.

Appendix

reaction pathways: dissociationCb-iCa2 and Cb-iCb2?

Appendix

Publications

This Work:

- (1) Heiden, S.; Yue, Y.; Kirsch, H.; Wirth, J.; Saalfrank, P.; Campen, R. K.: »title«,
Journal year, vol, pp.
- (2) Heiden, S.; Saalfrank, P.: »title«, *Journal year*, vol, pp.

References

References

Erklärung

Hiermit versichere ich, dass die vorliegende Arbeit an keiner anderen Hochschule eingereicht sowie selbständig und ausschließlich mit den angegebenen Mitteln angefertigt worden ist.

Potsdam, xx 2018